Genetic-based optimization of a multi insulator tunneling diode for THz energy harvesting

Mazen Shanawani [iD], Diego Masotti and Alessandra Costanzo [iD]

Department of Electrical, Electronic and Information Engineering, Edificio Storico, via. del Risorgimento 2, 40136, Bologna, Italy

Research Article

Abstract

The deployment of multi-insulator tunneling diodes has recently had more attention to be used as rectifiers in energy harvesting rectennas with good potentiality for a millimeter and terahertz range. However, with the rather complicated math to obtain the current–voltage relation, it is difficult to evaluate the design figures of merit (FOM)s such as asymmetry, non-linearity, responsivity, and dynamic resistance and monitor the impact of changing physical parameters on them. This complicates the decision-making process for the required physical parameters. In this work, a heuristic optimization framework using genetic algorithm is suggested using the transfer matrix method to find the combination of physical parameters which satisfies the minimum required FOM set by users and weighted by their preference.

Introduction

The increasing popularity of the internet of things concept has been backed by the continuous development of networking terminals. Thanks to the improving technology, they are getting smaller, more efficient and cheaper. This development, however, puts forward the necessity to operate them without batteries. Furthermore, new communication standards suggest moving to millimeter frequency bands in order to host the increasing demand for ubiquitous communication networks. Today, it is frequently said that frequencies up to the 100 GHz band for the fifth generation (5G) cellular networks will be used [1, 2].

It is important, therefore, to design rectifying antennas (rectennas) that harvest energy efficiently: this is a need for 5G networks, as energy harvesting at mm-wave frequencies is indicated among the pillars of future architectures [3, 4]; at the same time, the possibility to extend the rectennas capability to THz frequencies, would have a huge impact on the energy autonomy of IoT devices, thanks to the exploitation of sunlight and heat as high-frequency sources [5]. However, at millimeter and terahertz frequencies the current technology yields poor efficiency due to the poor figures of merits (FOMs) of the rectifying diode. Possible candidate diodes that have a rapid response are the tunneling diodes. As explained in [5] there are many types of them and for the sake of brevity we will focus on diodes made of single or multi-insulator structures laminated between two metal electrodes. Another advantage offered by multi-insulator diodes is their capability to reduce the junction capacitor effect and hence minimizing the linear current since they can be considered as series-connected capacitors [6]. However, achieving the best balance between the targeted design FOM and the good choice of materials and their thicknesses has always been a question [7].

To solve this problem, in this article we introduce this missing capability using a novel optimization approach that uses genetic algorithm (GA) to search for the optimum diode design parameters to give the best FOM values. To the best of our knowledge, this is the first time a heuristic approach is applied on a tunneling diode model to optimize its efficiency yield.

In the following section, a brief overview of the previous work on various tunneling models that has inspired the currently-presented optimization approach is presented. A detailed description of the developed optimization software structure is introduced in the system description section. The simulation results are demonstrated in the following section where the optimization is issued on two scenarios; a single insulator MIM diode scenario, and a double MIIM diode scenario with the obtained results. The conclusions are placed in the end with more discussion about the future steps and the adaptability of this optimization program for other tunneling models.

CAMBRIDGE
UNIVERSITY PRESS

Overview

As denoted in [5], there are many approaches used to model tunneling diodes. A recent work by Moulin *et al.* [4] reassured the fact that different models can have significantly different values for the $I(V)$ relation for the same physical input parameters. Solving the time-independent wave *Schrödinger's* equation accurately is critical to evaluate the functionality

of the tunneling diode. However, there is a trade off between an accurate solution of the wave equation (and hence an accurate $J(V)$ relation), and the required time and computer resources. It has been reported [8–10] and recently by [4] that transfer matrix method (TMM) offers very good compromise between accuracy and required time and resources. In fact, the work of [11] and [12] shows noticeably better performance for two insulator (MIIM) tunneling diodes with significantly improved FOMs. Conceptually, using two or more layers gives rise to: (a) enhanced tunneling phenomena such as resonant tunneling, step tunneling, and Fowler–Nordheim tunneling [9, 11]; (b) higher degrees of freedom for the design problem; and (c) decreased junction capacitor value based on series-connected capacitors [6]. Thus, we get enhanced and better controlled nonlinearity (that is, more control over FOM), and decreased linearity resulting from the junction series-capacitor effect. In light of that, it would be beneficial to *systematically* search for the best compromise between the used materials and the best *performance* as set by the user.

System description

Out of many optimization algorithms frequently used in the literature, we choose the GA due to its heuristic nature. Furthermore, it does not need to find the derivative for the objective function. The last point is important to handle the complicated wave function that has a less-predictable dependence on a series of integral/differential calculations starting from FOMs, and involving current density integrals, and complex inverse matrix calculations to solve the TMM system.

Another reason is the discrete nature of the solution space that can be easily managed by GA, differently from other optimization strategies: this need comes from the types of metals and insulators that are identified by indexes as well as their thicknesses which are assumed to be multiples of 0.1 nm. This assumption is based on the fact that the atomic diameter for metals in many cases exceed 0.1 nm [13].

The software is made from two nested-loop procedure; the outer (optimization) loop and the inner (solution and objective function) loop. In the data input, the program reads a list of possible solution metals and insulators names and parameters, targeted FOM values, their priorities based on a user-defined weighting value, and all the necessary information to control the functionality of the GA. The program, then, invokes another set of programs adapted from [14] which utilizes the TMM to evaluate the tunnel diode $J(V)$ relationship. Based on the found $J(V)$ all FOMs are calculated as introduced in [5]. The objective function evaluates the cost value to address the outer (optimization) loop to go on.

As shown in Fig. 1 the optimizer system is made of several functions which communicate with each other to provide the required information to the GA that searches for the solution. The data is presented to the system in terms of a simple ASCII file. This file contains all the physical parameters needed to run the optimization such as metal work functions, effective mass, insulators electron affinities, dielectric constant, etc. It is also responsible to define the possible solution space X to search for *at least good enough* solution. This solution space is presented to the GA in terms of upper and lower boundary values to search within by the GA. In order to search for the solution the GA throws the kth possible candidate solution to the objective function in the form of a vector $x_k \in X$. The objective function invokes the TMM for every voltage set by the user already imported from

the data input file and gets the corresponding current value. The fitness value function is evaluated according to (1).

$$C(x_k) = \sum^{p=\{\alpha, \chi, \gamma, R_D\}} w_p \frac{|tr_p - P_{kp}(x_k)|}{tr_p} SF_p \qquad (1)$$

where $C(x_k)$ is the objective function value output for the kth instance, $\mathbb{P} = \alpha, \chi, \gamma, R_D$ is the set of FOMs targeted for optimization which are asymmetry, nonlinearity, responsivity, and dynamic resistance, respectively. These values are a function of the corresponding voltage. However, the program takes just the maximum value and calculates the corresponding objective function shown in (1). For each optimization target $p \in \mathbb{P}$, the function will evaluate the cost by finding the value for the kth instance of the pth FOM $P_{kp}(x_k)$. The cost is simply the normalized absolute difference between the found value $P_{kp}(x_k)$ and the target value read from the optimizer input file tr_p. The contribution of this cost is then weighted by the value read from the optimizer input file w_p. SF_p represents a step function for the pth FOM which always takes the value 1 until the corresponding target is equal to or larger than the target value tr_p (having higher FOM is even better), and so the objective function is minimized. The only exception is the value of the dynamic resistance R_D where SF_p is negated to favor *lower* resistance values.

The system is built to host for the optimization process up to *three* intermediate layers between the metal electrodes (i.e., MIIIM diode). This necessitates a 9-dimensional space to search in for the solution. In other words, each vector instance x_k has nine components that identify the number of insulating layers, the left electrode metal identifier, right electrode metal identifier, first insulator identifier, first insulator thickness, second insulator identifier, second insulator thickness, third insulator identifier, and third insulator thickness. All the components *including thicknesses* are integers. Identifiers and number of layers are necessarily integers. However, the thickness component represents thicknesses in multiples of 0.1 nm which would be enough accuracy because it is the same order of magnitude as for atom diameters.

It is out of the scope of this paper to explain the TMM as it has been done by many others [8, 15–17]. However, it is worthwhile to mention that the technique followed in [9] has given accurate results against many practical experiments. That work accounts for the image force lowering effect. In comparison with the Simmons model [9, 18] utilizes a single electron model when this effect is calculated. Furthermore, a proprietary adaptive mesh model is adopted to divide the insulator medium into slices with different thicknesses and find the corresponding voltage level for each slice. Figure 2 shows the reproduced potential profile for the parameters taken from [11] for a Al–4 nmNb$_2$O$_5$–1 nmAl$_2$O$_3$–Al MIIM diode after applying a 0.3 V bias voltage. Evidently, the profile is not equally sliced across the whole range due to the adaptive mesh approach. Also, with respect to [11] the effect of image force lowering causes the chamfered corners of the profile as shown in Fig. 2. This lowering effect reduces the average barrier thickness that the tunneling electron has to traverse, and so increases the tunneling current value *subject to the solution of Schrödinger's time-independent equation.* Then, the potential value at each slice interface – with the corresponding thickness of each slice – is fed into the TMM method to find the tunneling electron transmission probability $T(E_x)$ along x which is used to evaluate the tunneling current value. Solving the TMM model is based on the near-diagonal square matrix method [19] which is claimed to minimize the rounding errors and provide numerical stability.
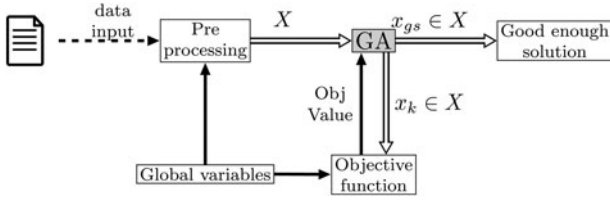
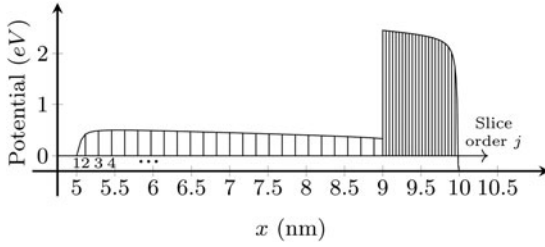**Fig. 1.** Schematic diagram of the optimization program used.

Fig. 2. Potential profile of an example MIIM diode made of Al–4 nmNb_2O_5–1 nmAl_2O_3–Al as calculated by [14] with image forces included. The vertical lines show the borders between slices.

Simulation results

Input parameters

Table 1 shows two scenarios which have been tried in the process to evaluate the system performance. For each scenario, there is a group of metals which consists of one or more metals and each metal is represented by its work function value Ψ. Similarly, the scenario also contains a group of one or more insulators which are represented by their electron affinity χ, and dielectric constant K. The first scenario assumes a single insulator diode formed from niobium nitride NbN, and niobium metal electrodes, and in between a niobium oxide Nb_2O_5 layer is assumed and is based on the parameters used in [9]. The optimizer tries also different thicknesses ranging from 0.1 to 3 nm with 0.1 nm step size. Scenario 2 is for an MIIM diode with aluminum metal electrodes: the choice of metals, insulators, and insulating thicknesses is made by the optimizer to minimize the objective function output. It should be reported that Ψ and χ values are experiment-dependent and can considerably vary based on the experiment and the interfacing medium and hence can greatly affect the potential profile and the resulting response [9]. Therefore, the values of Scenario 2 have been set to reproduce the same voltage profile in [11] with the thickness varying from 0.8 to 2.8 nm with 0.1 nm step. For each population of individuals the GA tries different combinations of metals and insulators chosen from their corresponding groups, and varies the thickness of oxide layers in order to minimize the output of (1).

The model also adopts the target values tr_p and their respective weights w_p for both scenarios as shown in Table 2. The FOMs have been evaluated based on a straightforward approach using difference between subsequent $J(V)$ points to evaluate dJ. This approach results in reducing the number of points by one for each differentiation. When compared to their original values, averaging between successive points has been done to also reduce the number of total points by one.

Using the MATLAB® GA toolbox [20] with a population size of 30 individuals, function tolerance of 10^{-4}, and elite count 5 for both scenarios provides the results shown in Section "Results".

Table 1. Input parameters used for the GA optimizer in Scenario 1 (Sc. 1), and Scenario 2 (Sc. 2).

	Material	Property	Value
Sc. 1	Nb	Ψ	4.33 eV
	NbN	Ψ	4.7 eV
	Nb_2O_5	χ	4.23 eV
		K	25
Sc. 2	Al	Ψ	5 eV
	Nb_2O_5	χ	4.44 eV
		K	25
	Al_2O_3	χ	2.32 eV
		K	9.7

Table 2. Targeted FOM and the corresponding weights used for the GA optimizer.

		α	χ	γ		R_D
Sc. 1	tr_p	1.3	2.5	5	V^{-1}	3 kΩcm^2
	W_p	1	1	1		10
Sc. 2	tr_p	10	6	8	V^{-1}	500 Ωcm^2
	W_p	2	5	1		80

Table 3. Initial and final states of the GA run for the optimized scenarios.

	Initial	Final
Sc. 1	NbN–2 nmNb_2O_5–Nb	Nb–2.4 nmNb_2O_5–NbN
	[9]	
Sc. 2	Al–3 nmNb_2O_5–3 nmAl_2O_3–Al	Al–2.7 nmNb_2O_5–2 nmAl_2O_3–Al
	[11]	

Results

In order to calculate the FOM, the equations in [21] are used where the diode junction area can be simplified from the equations of α, χ, and γ and so it is not necessary to have it to calculate them. As shown in Table 3 the optimization of Scenario 1 advises to use Nb (NbN) metals for the left(right) electrodes, respectively, with a thickness of 2.4 nm of Nb_2O_5. In order to compare the results, the $J(V)$ curve of [9] has been reproduced using 7th order fitted polynomial. Due to the long time taken for each simulation, the optimized design has been simulated using a voltage range from −0.3 to 0.3 V with 0.1 V steps and the resulting $J(V)$ curve has been fitted by a 7th order polynomial to obtain a simple analytic description of the $J(V)$ relation. Using the obtained polynomials the FOM figures for both cases can be easily reproduced as shown in Fig. 3.

Although the reference case of [9] shows higher current density with respect to the reached model, the inset figure clearly shows improved results both for nonlinearity – which is supposed to be the most important FOM – and responsivity for all the voltage range extending from −0.3 to 0.3 V except for the values just around zero. This is attributed to the rapid transition between the
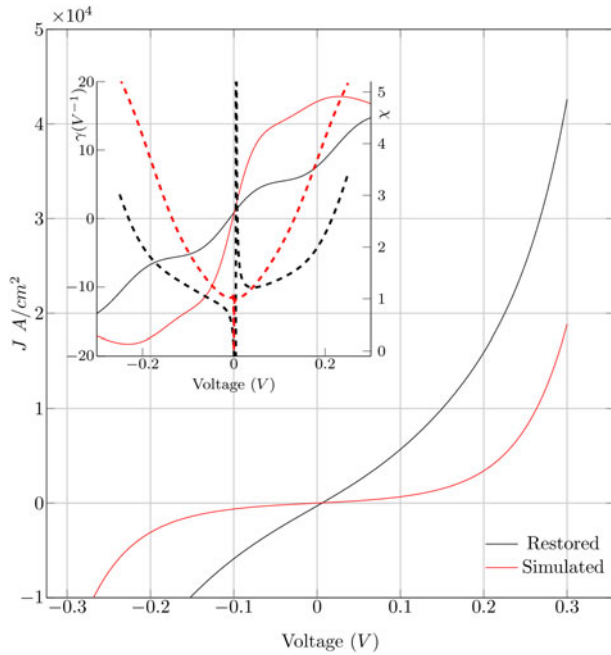
Fig. 3. $J(V)$ response of a single insulator diode as explained in Scenario 1. Red curves are the simulated results while black curves are the restored results from [9]. Solid lines in the inset figure represent responsivity γ while dashed lines represent nonlinearity χ.

Fig. 4. $J(V)$ response of a double insulator diode as explained in Scenario 2. Continuous curves are $J(V)$ curves of the restored results of [11]. The inset figure shows the solid and dashed curves of the restored response for responsivity γ and nonlinearity χ, respectively.

positive and negative parts. That improvement has been on behalf of reduced dynamic resistance value R_D which significantly increased. Having said that it remained well below the defined target in Table 2.

Table 3 also shows that the best available result of the optimization of Scenario 2 happens for the Al–2.7 $nmNb_2O_5$–2 $nmAl_2O_3$–Al structure which resulted in the curves shown in Fig. 4. The restored $J(V)$ curve from [11] is the solid black curve. The inset figure shows the restored and optimized results for χ in dashed lines, and γ in solid lines.

For the optimized case, both χ and γ show significant *ripples* in the positive half. Responsivity of the restored curve and the optimized case is of the same order of magnitude. Although the restored case shows noticeably higher γ in the positive half between 0.15 and 0.25 V, the optimized case experiences *ripples* with a varying γ between 6 and 20 V^{-1}. Both γ and χ values of the optimized case are higher in the negative half.

It is worth noting that the high difference in current densities between Scenario 1 and 2 may be attributed to the suboptimum choice of materials and their thicknesses.

Conclusions

In this work a software framework which can be useful for subsequent industrial steps has been presented. Although empirically expecting the value of responsivity for the MIIM diode is possible based on the estimated potential profile, taking account of many FOMs and the best decision making approach is difficult to reach using simplified approaches. With the presented technique the user can set the desired FOM values and their respective weights and let the GA look for the qualified solutions.

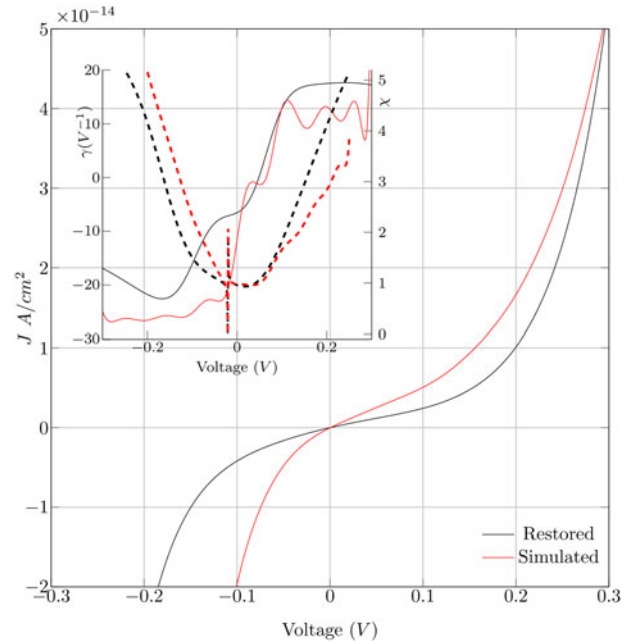The double insulator would possibly offer better results with respect to single insulator structure when using proper materials and thicknesses. The obtained optimization results have shown significant improvements in the case of a MIM diode and limited ones in the multi-insulator case. However, these results represent a first trial by just varying the insulator thicknesses with a limited set of metals and insulators. By increasing the number of these design parameters, reaching improved design and performance is much more probable.

It is also worth noting that there are more articulated models that take into account more complicated tunneling mechanism such as Kane, Karlovsky, and band to band tunneling [4]. In principle, the optimization solution presented here is ready to adopt these models and it can be beneficial to compare the optimization output for these models.

The program now looks for the maximum FOM value achieved in a specific voltage range: for future releases, the user might wish to be more specific and optimize a FOM at a specific voltage point, thus having a more agile analysis.

References

1. **5GAmericas** (2017) White paper on 5g spectrum recommendations. Available at https://www.5gamericas.org/wp-content/uploads/2019/07/5GA_5G_Spectrum_Recommendations_2017_FINAL.pdf.
2. **Arrow Magazine** (2019) What frequency spectrum will 5G technology use and how does this compare to 4G?. Available at https://www.arrow.com/en/research-and-events/articles/what-frequency-spectrum-will-5g-technology-use-and-how-does-this-compare-to-4g.

3. **Hossain E, Rasti M, Tabassum H and Abdelnasser A** (2014) Evolution toward 5g multi-tier cellular wireless networks: an interference management perspective. *IEEE Wireless Communications* **21**, 118–127. ISSN 1558-0687.

4. **Moulin N, Amara M, Mandorlo F and Lemiti M** (2019) Tunnel junction I(V) characteristics: review and new model for p-n homojunction. *Journal of Applied Physics* **126**, 033105.

5. **Shanawani M, Masotti D and Costanzo A** (2017) THz rectennas and their design rules. *Electronics* **6**, 99.

6. **Hayt WH and Buck JA** (2001) *Engineering Electromagnetics*, vol. **6**. McGraw-Hill, New York.

7. **Moddel G** (2013) Will rectenna solar cells be practical? In Moddel G and Grover S (eds), *Rectenna Solar Cells*. New York, NY: Springer, pp. 3–24.

8. **Ghatak AK, Thyagarajan K and Shenoy MR** (1988) A novel numerical technique for solving the one-dimensional Schrodinger equation using matrix approach-application to quantum well structures. *IEEE Journal of Quantum Electronics* **24**, 1524–1531.

9. **Grover S and Moddel G** (2012) Engineering the current–voltage characteristics of metal–insulator–metal diodes using double-insulator tunnel barriers. *Solid-State Electronics* **67**, 94–99.

10. **Hashem IE, Rafat NH and Soliman EA** (2013) Theoretical study of metal-insulator-metal tunneling diode figures of merit. *IEEE Journal of Quantum Electronics* **49**, 72–79.

11. **Mitrovic IZ, Weerakkody AD, Sedghi N, Hall S, Ralph JF, Wrench JS, Chalker PR, Luo Z and Beeby S** (2016) Tunnel-barrier rectifiers for optical nantennas. *ECS Transactions* **72**, 287–299.

12. **Herner SB, Belkadi A, Weerakkody A, Pelz B and Moddel G** (2018) Responsivity–resistance relationship in MIIM diodes. *IEEE Journal of Photovoltaics* **8**, 499–504.

13. **Slater JC** (1964) Atomic radii in crystals. *The Journal of Chemical Physics* **41**, 3199–3204.

14. **Grover S** (2013) Metal-insulator diode simulator. Available at http://ecee.colorado.edu/~moddel/QEL/MIMDiodeSim.zip.

15. **Jonsson B and Eng ST** (1990) Solving the Schrödinger equation in arbitrary quantum-well potential profiles using the transfer matrix method. *IEEE Journal of Quantum Electronics* **26**, 2025–2035. ISSN 0018-9197.

16. **Li W** (2010) Generalized free wave transfer matrix method for solving the Schrödinger equation with an arbitrary potential profile. *IEEE Journal of Quantum Electronics* **46**, 970–975. ISSN 0018-9197.

17. **Pujol O, Carles R and Pérez J-P** (2014) Quantum propagation and confinement in 1d systems using the transfer-matrix method. *European Journal of Physics* **35**, 035025.

18. **Simmons JG** (1963) Generalized formula for the electric tunnel effect between similar electrodes separated by a thin insulating film. *Journal of applied physics* **34**, 1793–1803.

19. **Probst OM** (2002) Tunneling through arbitrary potential barriers and the apparent barrier height. *American Journal of Physics* **70**(11), 1110–1116.

20. **The MathWorks, Inc** (2018) MATLAB R2018b Optimization Toolbox 8.1. Available at https://uk.mathworks.com/help/gads/genetic-algorithm.html.

21. **Aldrigo M, Dragomir M, Modreanu M, Povey I, Iordanescu S, Vasilache D, Dinescu A, Shanawani M and Masotti D** (2018) Harvesting electromagnetic energy in the *V*-band using a rectenna formed by a bow tie integrated with a 6-nm-thick au/hfo2/pt metal–insulator–metal diode. *IEEE Transactions on Electron Devices* **65**, 2973–2980. ISSN 0018-9383.

Mazen Shanawani received the M.Sc. degree in communication systems and signal processing from the University of Bristol, Bristol, U.K. He had worked in the Arab International University (AIU) in Syria for until 2016 before he won the scholarship to complete the Ph.D. studies at the University of Bologna, Italy. He is currently pursuing the Ph.D. degree in the millimeter and terahertz rectennas where the Ph.D. program aims to find more accurate ways for simulation and industrialization of high-frequency diodes to pave the way for more efficient energy harvesting devices at higher frequencies. He has recently won the EnABLES support for a proposal to fabricate optimized nonlinear high-frequency diodes in order to fabricate optimized prototypes. His research interests include: co-simulation and optimization of linear and nonlinear energy harvesters, energy-efficient antenna arrays, and modeling of tunneling devices.

Diego Masotti (M'00, SM'16) received the Ph.D. degree in electric engineering from the University of Bologna, Italy, in 1997. In 1998 he joined the University of Bologna as a Research Associate of electromagnetic fields. His research interests are in the areas of nonlinear microwave circuit simulation and design, with emphasis on nonlinear/electromagnetic co-design of integrated radiating subsystems/systems for wireless power transfer and energy harvesting applications. He authored more than 60 scientific publications on peer reviewed international journals and more than 100 scientific publications on proceedings of international conferences. Dr. Masotti serves in the Editorial Board of the International Journal of Antennas and Propagation, of the Cambridge journal of Wireless Power Transfer, of IEEE Access, and he is a member of the Paper Review Board of the main Journals of the microwave sector.

Alessandra Costanzo (A'99–M'02–SM'13) is a Full Professor with the University of Bologna, Italy. She has authored more than 200 publications and several chapter books. Her research interests include CAD for co-design and modeling of active nonlinear microwave/RF circuits. She has proposed novel solutions for energy-autonomous RF systems based on the wireless power transmission, adopting both far-field and near-field solutions, for several power levels and operating frequencies. She is a member of the MTT-24 RFID. She is the Past-Chair of the MTT-26 on Wireless Energy Transfer and Conversion. She was a co-founder of the EU COST Action IC1301 WiPE. She is the MTT-S Representative and Distinguished Lecturer of the IEEE CRFID. She is Steering Committee Chair of the IEEE JOURNAL OF RADIO FREQUENCY IDENTIFICATION. She is Associate Editor for IEEE TRANSACTIONS ON MICROWAVE THEORY AND TECHNIQUES, for the Cambridge Journals of Microwave and Wireless Technologies, and of Wireless Power Transfer.